Pump-wave effects on the propagation of noisy signals in nonlinear dispersive media

M. Yu

Department of Mechanical Engineering, University of Rochester, Rochester, New York 14627, and Laboratory for Laser Energetics, 250 East River Road, Rochester, New York 14623

G. P. Agrawal

The Institute of Optics, University of Rochester, Rochester, New York 14627

C. J. McKinstrie

Department of Mechanical Engineering, University of Rochester, Rochester, New York 14627, and Laboratory for Laser Energetics, 250 East River Road, Rochester, New York 14623

Received September 22, 1994; revised manuscript received January 12, 1995

Stochastic field propagation in nonlinear dispersive media is studied in the undepleted-pump approximation in both the normal- and the anomalous-dispersion regimes. A statistical description of modulational instability is given in the anomalous-dispersion regime. Nonlinear dispersive effects are present even in the normal-dispersion regime. Analytical results are obtained for the evolution of the power spectrum and the relative intensity noise and are confirmed by numerical simulations. The results are applied to the four-wave mixing of broadband signals in nonlinear dispersive media.

1. INTRODUCTION

When a partially coherent electromagnetic field propagates through a medium, its coherence properties usually change.[1–7] More specifically, the output power spectrum and relative intensity noise (RIN) may differ substantially from the input power spectrum and RIN associated with the stationary stochastic field. Transformation between the input and the output power spectra is a basic statistical property for many systems. For a linear system the spectral transformation is related to the impulse-response function and can be calculated easily by use of the Wiener–Khinchin theorem.[8,9] In this paper we consider an optical field propagating through a single-mode optical fiber used as an example of a nonlinear dispersive medium. The deterministic transformation of the input signal, in this case an optical field, is governed by a nonlinear Schrödinger equation (NSE), which takes into account group-velocity dispersion (GVD) and the Kerr-type nonlinearity responsible for self-phase modulation [see Eq. (1) below].[10,11] Thus the statistical properties of the output signal, such as the power spectrum and the RIN, are determined not only by the statistics of the input signal but also by the dispersive and nonlinear properties of the fiber.[2]

In such systems there exists an intrinsic frequency for a given average power of propagation that permits a direct comparison between the dispersive and nonlinear terms in the NSE. This frequency corresponds to the peak gain frequency of modulational instability (MI) in the anomalous-dispersion regime[10,11] and is also a useful parameter in the normal-dispersion regime. Here the power used for calculating this frequency refers to the average power of the stationary stochastic field. If the spectral width is much larger that this intrinsic frequency, the nonlinear term can be neglected and the system can be considered linear. It is easy to see that the Wiener–Khinchin theorem predicts no change in the power spectrum in this case. On the other hand, the dispersive term can be neglected if the spectral width is much smaller than this intrinsic frequency. For systems with negligible dispersion the problem of spectral evolution has been studied for an input field with Gaussian statistics.[1]

Generally, the coexistence of dispersion and self-phase modulation makes the problem of stochastic propagation impossible to study analytically.[2] If, however, the input consists of a continuous-wave (cw) field plus a small noise field whose amplitude is much smaller than that of the cw field, a linearization technique can be applied to analyze the problem, with the small part treated as perturbation. This case is considered in detail in the following sections, where analytical expressions for the evolution of the power spectrum and the RIN are given and are confirmed by numerical simulation. It should be pointed out that the linearization method was first developed to study squeezing in quantum optics.[12–14] Here we concerned ourselves with the classical case.

In the spectral domain the situation described above corresponds to an input power spectrum that consists of a δ-function portion plus a small part whose area is much smaller than the area of the δ-function portion. In practice our analysis applies to a laser light with a small component of broadband background noise. It can also

0740-3224/95/061126-07$06.00

be applied to the case of four-wave mixing[11] (FWM) of a partially coherent (broadband) signal in the presence of a cw pump. Because without the small perturbation the cw pump spectrum is unchanged, the linearization method used here gives only the pump effects on the propagation of a partially coherent field in a nonlinear dispersive medium. It is well known that MI occurs in the anomalous-dispersion regime. Thus our results will provide a statistical description of MI.

2. NOISE PROPAGATION

The governing NSE can be written as[11]

$$\partial_z A = -\frac{i}{2}\beta_2 \partial_{tt}{}^2 A + i\gamma|A|^2 A, \tag{1}$$

where A is the complex field amplitude, z is the propagation distance, t is the retarded time measured in a frame moving at the group velocity, β_2 is the GVD coefficient, and γ is the nonlinear coefficient. To simplify the notation, we will often use $\beta \equiv \beta_2/2$ in what follows. The input field is assumed to be $A(t, 0) = A_0 + \delta A(t, 0)$, where $|\delta A(t, 0)| \ll |A_0|$. To the zeroth order (without noise) we have the solution $A_s(t, z) = A_0 \exp(i\gamma|A_0|^2 z)$. Thus we assume a solution of the form $A(t, z) = A_s + \delta A_s = [A_0 + \delta A(t, z)]\exp(i\gamma|A_0|^2 z)$ and linearize Eq. (1) in the small perturbation δA to obtain the linear partial differential equation

$$\partial_z \delta A = -i\beta\partial_{tt}{}^2\delta A + i\gamma(|A_0|^2\delta A + A_0{}^2\delta A^*). \tag{2}$$

The solution to Eq. (2) is easily expressed in the Fourier domain. By taking the Fourier transforms of the above equation and its complex conjugate, we have

$$\begin{aligned} &\mathrm{d}_z\overline{\delta A}(\omega, z) - i\beta\omega^2\overline{\delta A}(\omega, z) - i\gamma|A_0|^2\overline{\delta A}(\omega, z) \\ &\qquad = i\gamma|A_0|^2 A_0{}^2\overline{\delta A}^*(-\omega, z), \\ &\mathrm{d}_z\overline{\delta A}^*(-\omega, z) + i\beta\omega^2\overline{\delta A}^*(-\omega, z) + i\gamma|A_0|^2\overline{\delta A}^*(-\omega, z) \\ &\qquad = -i\gamma|A_0|^2 A_0{}^2\overline{\delta A}(-\omega, z), \end{aligned} \tag{3}$$

where $\overline{\delta A}$ refers to the Fourier transform of δA [i.e., $\overline{\delta A}(\omega) = \int_{-\infty}^{\infty} \delta A \exp(i\omega t)\mathrm{d}t$]. Equations (3) show that the basic physics is related to FWM that causes coupling between the two sidebands $\overline{\delta A}(\omega, z)$ and $\overline{\delta A}^*(-\omega, z)$ located symmetrically around the cw pump frequency.

It is easy to obtain the general solution of the above coupled, linear, first-order, ordinary differential equations. For each ω there are two independent solutions. Thus, in terms of the two eigenmodes, the general solution is given by

$$\begin{aligned} \begin{bmatrix} \overline{\delta A}(\omega, z) \\ \overline{\delta A}^*(-\omega, z) \end{bmatrix} &= c_1 \begin{bmatrix} 1 \\ r_+ \end{bmatrix} \exp(ik_+ z) \\ &\quad + c_2 \begin{bmatrix} r_- \\ 1 \end{bmatrix} \exp(ik_- z), \end{aligned} \tag{4}$$

where c_1 and c_2 are constants and $k_\pm$ and $r_\pm$ are defined as

$$k_\pm(\omega) = \pm[(\gamma|A_0|^2 + \beta\omega^2)^2 - (\gamma|A_0|^2)^2]^{1/2}, \tag{5}$$

$$\begin{aligned} r_+(\omega) &= \frac{k_+(\omega) - \beta\omega^2 - \gamma|A_0|^2}{\gamma A_0{}^2} \\ &= -\frac{\gamma A_0{}^{*2}}{k_+(\omega) + \beta\omega^2 + \gamma|A_0|^2}, \end{aligned} \tag{6}$$

$$\begin{aligned} r_-(\omega) &= \frac{\gamma A_0{}^2}{k_-(\omega) - \beta\omega^2 - \gamma|A_0|^2} \\ &= -\frac{k_-(\omega) + \beta\omega^2 + \gamma|A_0|^2}{\gamma A_0{}^{*2}}. \end{aligned} \tag{7}$$

Here $r_\pm(\omega)$ are the relative amplitudes of the sidebands $\overline{\delta A}(\omega, z)$ and $\overline{\delta A}^*(-\omega, z)$ for each eigenmode and $k_\pm(\omega)$ represents the corresponding dispersion relation.

If the field at the input $z = 0$ is known, Eq. (4) can be used to determine the two constants c_1 and c_2, and the field at any distance later can be expressed in terms of the input. After some straightforward algebra, we obtain

$$\begin{aligned} \begin{bmatrix} \overline{\delta A}(\omega, z) \\ \overline{\delta A}^*(-\omega, z) \end{bmatrix} &= \begin{bmatrix} M_{11}(\omega, z) & M_{12}(\omega, z) \\ M_{21}(\omega, z) & M_{22}(\omega, z) \end{bmatrix} \\ &\quad \times \begin{bmatrix} \overline{\delta A}(\omega, 0) \\ \overline{\delta A}^*(-\omega, 0) \end{bmatrix}, \end{aligned} \tag{8}$$

where

$$\begin{aligned} M_{11} &= [\exp(ik_+ z) - r_+ r_- \exp(ik_- z)]/(1 - r_+ r_-), \\ M_{12} &= r_-[\exp(ik_- z) - \exp(ik_+ z)]/(1 - r_+ r_-), \\ M_{21} &= r_+[\exp(ik_+ z) - \exp(ik_- z)]/(1 - r_+ r_-), \\ M_{22} &= [\exp(ik_- z) - r_+ r_- \exp(ik_+ z)]/(1 - r_+ r_-). \end{aligned} \tag{9}$$

3. POWER SPECTRUM OF THE FIELD

From the Wiener–Khinchin theorem,[8] the power spectrum $S(\omega, z)$, defined as the Fourier transform of the autocorrelation of the field, can be calculated as

$$\begin{aligned} S(\omega, z) &= \langle|\overline{A_s} + \overline{\delta A_s}|^2\rangle/T \\ &= \langle|\overline{A_s}|^2\rangle/T + \langle\overline{A_s\delta A_s}^* + \overline{A_s}^*\overline{\delta A_s}\rangle/T + \langle|\overline{\delta A_s}|^2\rangle/T \\ &= |A_0|^2\delta(\omega) + \langle|\overline{\delta A}(\omega, z)|^2\rangle/T, \end{aligned} \tag{10}$$

where the time window T extends to infinity in the limit. The cross term vanishes after averaging because $\overline{A_s}$ can be moved out of the average and $\langle\delta A_s\rangle = 0$.

Define $\Delta S(\omega, z) \equiv S(\omega, z) - |A_0|^2\delta(\omega)$, i.e., remove the unchanged portion of the spectrum corresponding to the cw signal. As $\overline{\delta A}(\omega, z)$ can be calculated from Eq. (8), we have

$$\begin{aligned} \Delta S(\omega, z) &= \langle|M_{11}\overline{\delta A}(\omega, 0) + M_{12}\overline{\delta A}^*(-\omega, 0)|^2\rangle/T \\ &= |M_{11}|^2\Delta S(\omega, 0) + |M_{12}|^2\Delta S(-\omega, 0), \end{aligned} \tag{11}$$

where we have assumed that $\langle\overline{\delta A}(\omega, 0)\overline{\delta A}(-\omega, 0)\rangle/T = 0$ or $\langle\delta A(t, 0)\delta A(t + \tau, 0)\rangle = 0$, which is true in most of the cases. Equation (11) is a linear transformation between the spectra, ΔS, at the output and the input. Both sidebands participating in the FWM process contribute to the output.

After further simplification, the output spectrum is given by

$$\Delta S(\omega, z) = \Delta S(\omega, 0) + (\gamma|A_0|^2)^2[\Delta S(\omega, 0) + \Delta S(-\omega, 0)] \times \sin^2[k(\omega)z]/[k(\omega)]^2, \quad (12)$$

where k is given by Eq. (5) regardless of the sign convention. Notice that when k is imaginary, which corresponds to MI, $\sin^2[k(\omega)z]/k^2(\omega) = (1/4)[\exp(|k|z) - \exp(-|k|z)]^2/|k|^2$.

Equation (12) predicts no spectral change in the limit of weak pump power, consistent with the result for a linear dispersive system. In the limit of zero dispersion Eq. (12) becomes

$$\Delta S(\omega, z) = \Delta S(\omega, 0) + (z\gamma|A_0|^2)^2 \times [\Delta S(\omega, 0) + \Delta S(-\omega, 0)], \quad (13)$$

which is valid as long as z is small enough that the noise power remains much smaller than the pump power.

Figures 1 and 2 display the output spectrum at different distances for the symmetric input spectrum for the cases of normal and anomalous dispersion, respectively. Notice that even in the normal-dispersion region, where MI does not occur, the nonlinear dispersive effects greatly affect the spectral evolution. From Eq. (12), the spectral intensity at any frequency is oscillating with distance (except at zero frequency, where it grows as z^2) because of the factor $\sin^2[k(\omega)z]/[k(\omega)]^2$. The period is $1/k(\omega)$, which is longer for smaller frequency and goes to infinity at the zero frequency. Thus the frequency components around zero keep growing, while fringes will be formed on the spectrum. For a fixed distance the power spectrum is an oscillating function of frequency, and the oscillations become faster at larger distances [see Eq. (12) and also Fig. 9 below]. The formation of the fine fringes indicates a long correlation time in a sense (because the autocorrelation of the field is just the Fourier transform of this spectrum) even if it is short at the input. This is an interesting statistical phenomenon inasmuch as it seems to indicate that the input field becomes more coherent on propagation because of pump-induced FWM. The quadratic growth of the field spectrum near zero frequency where the dispersion is negligible can also be explained in terms of self-phase modulation because the total field can then be written as $[A_0 + \delta A(t, 0)]\exp[i\gamma|A_0 + \delta A(t, 0)|^2 z] \simeq A_s + \delta A(t, 0)\exp(i\gamma|A_0|^2 z) + i\gamma A_0 z[A_0 \delta A(t, 0)^* + \text{c.c.}]$, where the term linear in z causes the quadratic power-spectrum growth.

In the anomalous-dispersion region and at large distances the exponential growth that is due to MI will dominate. Equation (12) for this case can be written as

$$\Delta S(\omega, z) = (\gamma|A_0|^2)^2[\Delta S(\omega, 0) + \Delta S(-\omega, 0)] \times \exp(2|k|z)/(2|k|)^2 \quad (14)$$

for large z. The output spectrum is symmetric independent of the symmetry of the input. If the input spectrum is broad enough (as in Fig. 2), the two peaks are at the frequency of the peak gain of MI, which is the maximum of $|k(\omega)|$ at $\omega = \pm(\gamma|A_0|^2/\beta)^{1/2}$. The linear approximation will eventually break down when the noise amplitude is comparable with the pump amplitude.

To confirm the validity of the linear approximation we have also performed numerical simulations by assuming Gaussian statistics[9] for the input field. Our

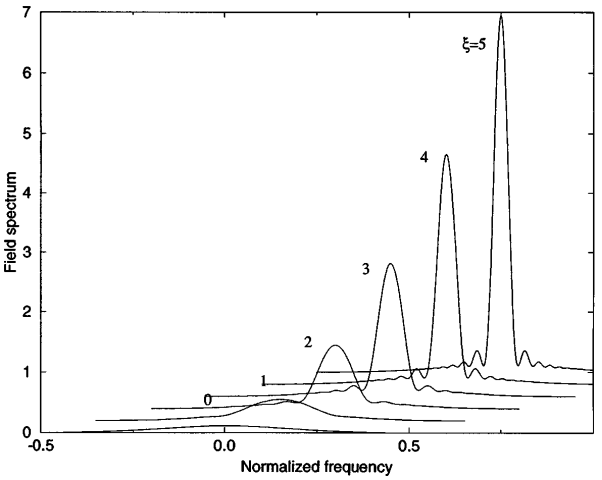

Fig. 1. Spectral evolution at different distances in the normal-dispersion region for a symmetric input spectrum. FWM causes the quadratic growth and fringe formations. The distance is normalized to $\xi = z\gamma|A_0|^2$, and the frequency is normalized as $\omega[|\beta|/(\gamma|A_0|^2)]^{1/2}/(4\pi)$. The FWHM of the input noise spectrum is 0.4, and its average intensity is 3.2×10^{-5} times the pump intensity. The vertical axis has a relative unit.

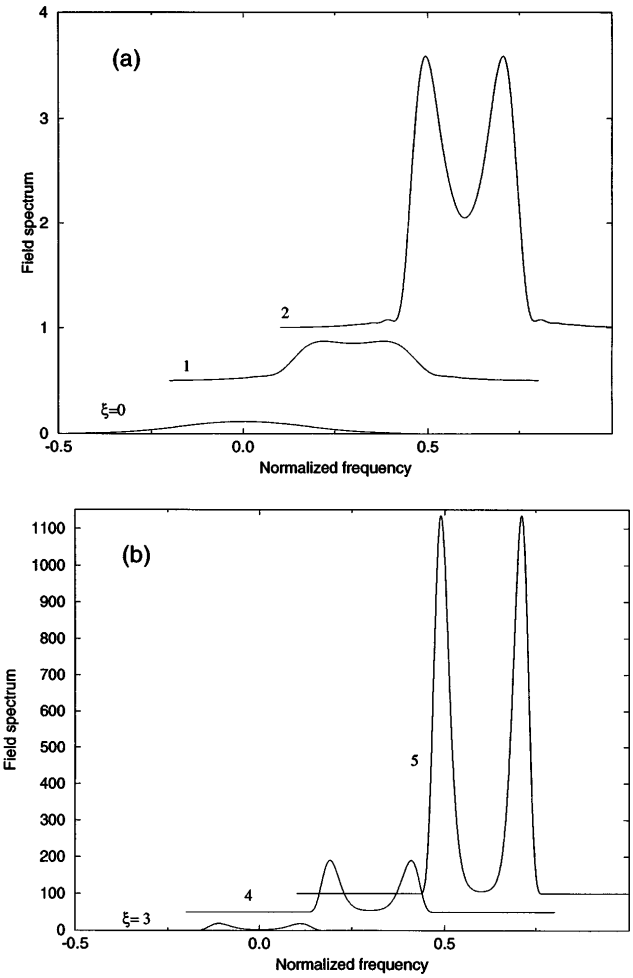

Fig. 2. Same as Fig. 1, except for the sign of the GVD parameter. MI effects dominate at a large distance.

numerical model is constructed as follows. For the noise field, two independent Gaussian random-number generators are used as the real and the imaginary parts of the input field, which is passed through a filter that determines the shape of spectrum. This noise field is added to the cw field to form the input field. We solve Eq. (1) for each preparation of the input, using the split-step Fourier method.[11] To avoid complications at the temporal boundaries, a broad Gaussian-pulse carrier is used whose width is much larger than the time scale of fluctuations, and the nonstationary effects introduced by the carrier are eliminated by application of a smaller (than the pulse width) window for calculating the power spectrum and the RIN. The results are averaged over 100 realizations by integration of the NSE 100 times.

Figures 3 and 4 are the spectral evolutions from our numerical simulations corresponding to Figs. 1 and 2. The analytical results agree with numerical simulations, although, because of MI, deviations begin to occur for large distances in the anomalous case when the amplitude of the noise field becomes comparable with the pump amplitude. The appearance of additional peaks on the spectrum, which are attributed to the higher-order FWM effect, indicates that our analytical treatment becomes invalid in this situation.

4. RELATIVE INTENSITY NOISE

Besides the autocorrelation or the power spectrum of the field, another quantity of statistical importance is the RIN. It is defined as the Fourier transform of the autocorrelation of the relative intensity fluctuation $\delta I/\langle I\rangle$ of the field, where $\delta I = I - \langle I\rangle$ and $I = |A|^2$ is the intensity. Thus it is related to the fourth-order moment of the stochastic field. In our case, $I = |A_0 + \delta A(t, z)|^2$. Consistent with the linear approximation, this leads to

$$\delta I(t, z)/\langle I\rangle = [A_0{}^*\delta A(t, z) + A_0\delta A^*(t, z)]/|A_0|^2 . \quad (15)$$

By use of the Wiener–Khinchin theorem, the RIN is given by

$$\mathrm{RIN}(\omega, z) = \langle |A_0{}^*\overline{\delta A}(\omega, z) + A_0\overline{\delta A}^*(-\omega, z)|^2\rangle/(T|A_0|^4) . \quad (16)$$

By using Eq. (8) we obtain

$$\begin{aligned}\mathrm{RIN}(\omega, z) &= |A_0{}^*M_{11} + A_0M_{21}|^2\langle|\overline{\delta A}(\omega, 0)|^2\rangle/(T|A_0|^4) \\ &\quad + |A_0{}^*M_{12} + A_0M_{22}|^2\langle|\overline{\delta A}(-\omega, 0)|^2\rangle/(T|A_0|^2) \\ &= |A_0{}^*M_{11} + A_0M_{21}|^2\Delta S(\omega, 0)/|A_0|^4 \\ &\quad + |A_0{}^*M_{12} + A_0M_{22}|^2\Delta S(-\omega, 0)/|A_0|^4 .\end{aligned} \quad (17)$$

Further simplification gives

$$\mathrm{RIN}(\omega, z) = |A_0|^{-2}[\Delta S(\omega, 0) + \Delta S(-\omega, 0)] \times \left\{1 - \frac{2\gamma|A_0|^2\sin^2[k(\omega)z]}{2\gamma|A_0|^2 + \beta\omega^2}\right\}, \quad (18)$$

where k is given by Eq. (5) regardless of the sign convention. From Eq. (18) we have $\mathrm{RIN}(\omega, 0) = |A_0|^{-2}[\Delta S(\omega, 0) + \Delta S(-\omega, 0)]$, indicating that the RIN is always symmetric at the input. The final result is thus given by

$$\mathrm{RIN}(\omega, z) = \mathrm{RIN}(\omega, 0)\left\{1 - \frac{2\gamma|A_0|^2\sin^2[k(\omega)z]}{2\gamma|A_0|^2 + \beta\omega^2}\right\}. \quad (19)$$

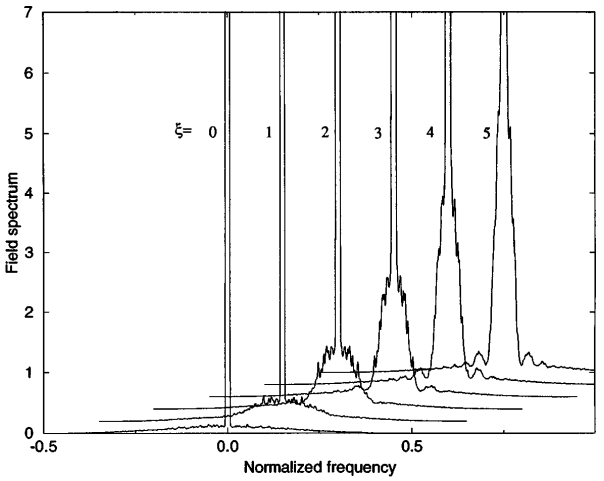

Fig. 3. Numerical simulation result corresponding to Fig. 1. The center portion is the cw spectrum subjected to finite resolution that is due to the temporal window for calculating the spectrum.

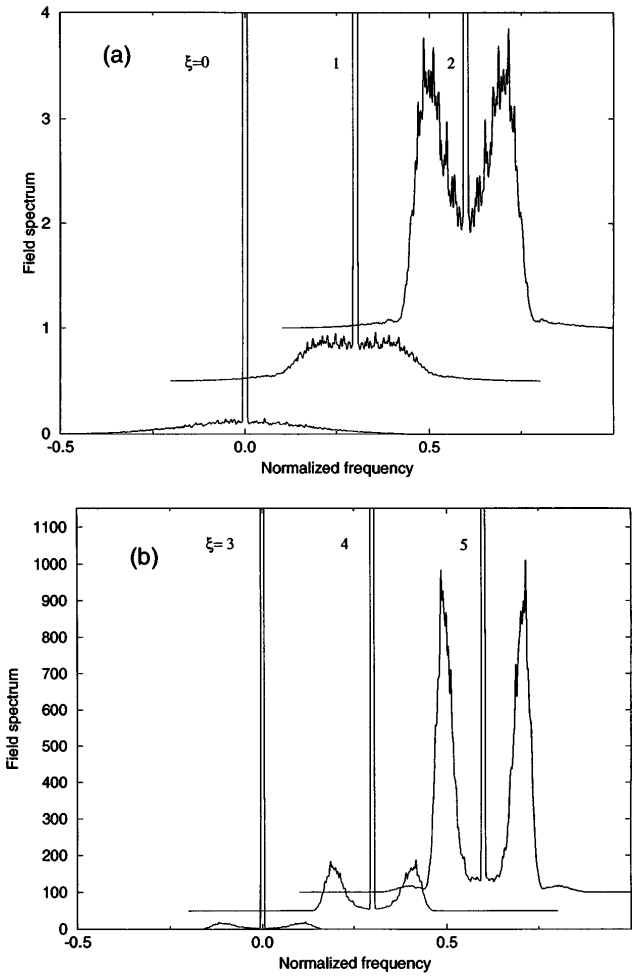

Fig. 4. Same as Fig. 3, except for the sign of the GVD parameter.

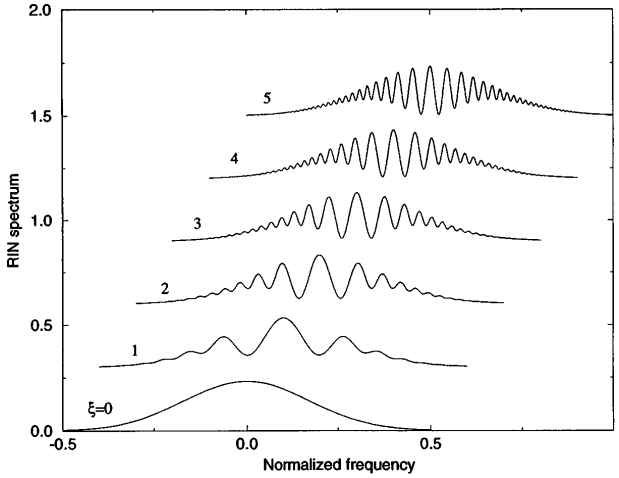

Fig. 5. Analytic RIN spectra at different distances in the normal-dispersion region under conditions identical to those of Fig. 1. FWM causes fringe formations.

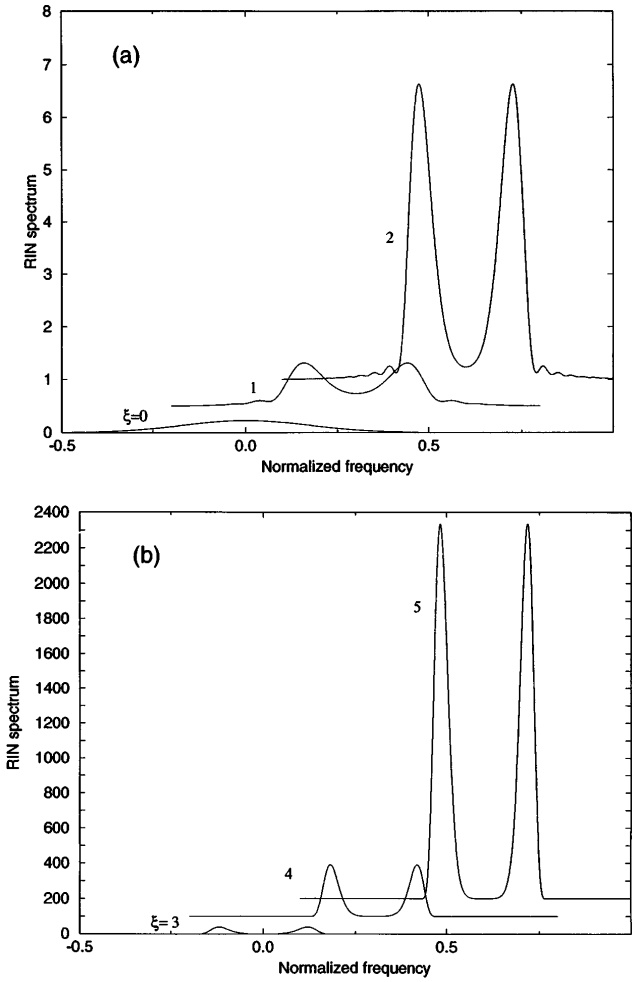

Fig. 6. Same as Fig. 5, except for the sign of the GVD parameter. MI effects dominate at a large distance.

This is a linear transformation between the RIN of the input and of the output. Equation (19) also predicts that, without nonlinearity or dispersion (i.e., $|A_0|^2 = 0$ or $\beta_2 = 0$), the RIN will not change (under our linear approximation).

Figures 5 and 6 show the evolution of the RIN corresponding to the cases of Figs. 1 and 2, respectively. Figures 7 and 8 are the corresponding numerical-simulation results. Like the power spectrum, even in the normal-dispersion region where no MI is present the nonlinear dispersive effects change the RIN. Because of the factor $\sin^2[k(\omega)z]/(2\gamma|A_0|^2 + \beta\omega^2)$ in Eq. (19) the RIN at

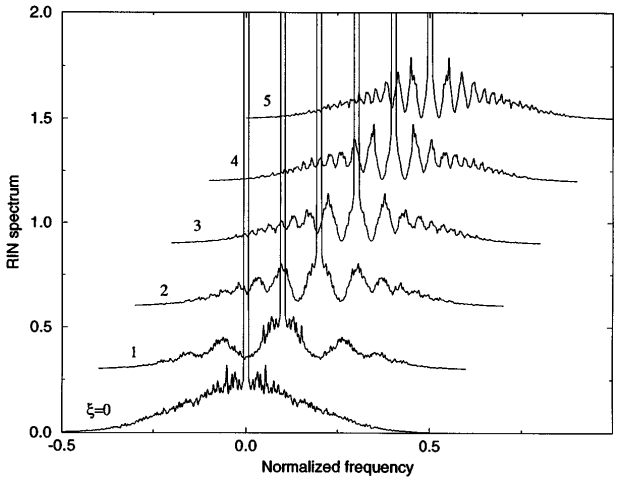

Fig. 7. Numerical simulation result corresponding to Fig. 5. The center portion is the cw residue.

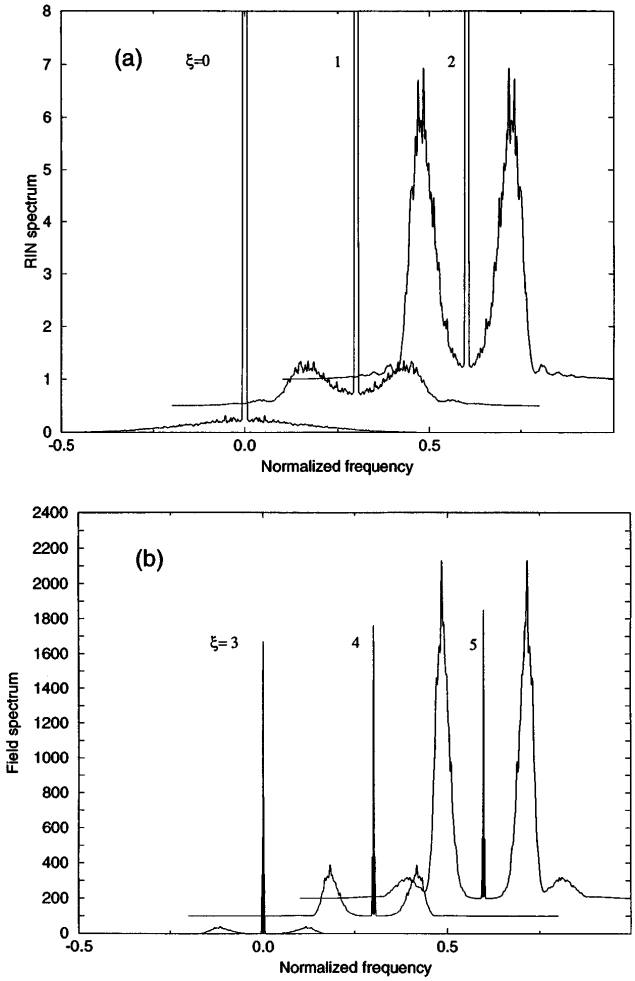

Fig. 8. Same as Fig. 7, except for the sign of the GVD parameter.

any frequency is oscillating with distance, except at zero frequency where the RIN is always unchanged. The period $1/k(\omega)$ is longer for smaller frequencies, and it goes to infinity at zero frequency. Thus the RIN at zero frequency is unchanged, while fringes will be formed at other frequencies. For a fixed distance the power spectrum is an oscillating function of frequency, and the oscillation becomes faster at larger distances. The numerical simulation confirms our analysis.

In the anomalous-dispersion region and at large distances the MI will dominate, because for large z Eq. (19) can be written as

$$\mathrm{RIN}(\omega, z) = \mathrm{RIN}(\omega, 0)\frac{\gamma|A_0|^2 \exp(2|k|z)}{4\gamma|A_0|^2 + \beta_2\omega^2}, \tag{20}$$

indicating an exponential increase that is due to MI gain. If the input spectrum is broad enough (as in Figs. 5–8), the two peaks are at the frequency of the peak gain of the MI, $\omega = \pm(2\gamma|A_0|^2/\beta_2)^{1/2}$. The linear approximation will eventually break down at extremely large z when the noise amplitude grows to be comparable with the pump amplitude. This is evident from the numerical simulation in which the appearance of additional peaks on the RIN is from a higher-order FWM effect.

5. NOISE-INDUCED FOUR-WAVE MIXING

FWM occurs when a cw pump and a weak signal or probe (usually with different carrier frequency) coexist in a nonlinear medium.[11] It has found many applications, including the use of its phase-conjugation effect to cancel the dispersive spreading of optical pulses in a fiber link for a broadband communication system.[15,16] In many cases it is important to understand the statistical properties of the fields after they undergo FWM, such as the shape of the field spectrum and the correlation time. Although it was developed in a different context, our formalism for the propagation of a stochastic field is well suited to describe the situation in FWM. In fact, Eq. (12) can be applied directly to the case of FWM in which a cw pump and a weak noisy or broadband probe are present at the input. In our linear approximation the cw pump is undepleted. Because Eq. (12) is a linear transformation between the spectrum of the nonpump part at the input and the output, we first consider a probe of narrow spectrum at ω' at the input, i.e., a form of δ function, $\Delta S(\omega, 0) = I_+(0)\delta(\omega - \omega')$, where $I_+(0)$ is a constant. From Eq. (12) we have

$$\Delta S(\omega, z) = I_+(z)\delta(\omega - \omega') + I_-(z)\delta(\omega + \omega'), \tag{21}$$

where

$$I_+(z) = I_+(0)\{1 + (\gamma|A_0|^2)^2 \sin^2[k(\omega')z]/[k(\omega')]^2\},$$
$$I_-(z) = I_+(0)(\gamma|A_0|^2)^2 \sin^2[k(\omega')z]/[k(\omega')]^2. \tag{22}$$

Equation (21) describes the FWM generation of the sideband at the idler frequency $-\omega'$ because of its coupling to the sideband at ω'.

Notice that in the weak-pump limit, i.e., $\gamma|A_0|^2 \ll |k(\omega')|$, the sideband at $-\omega'$ will not be generated because there is no coupling in this limit. In the case of the zero GVD the coupling behavior also changes, and Eq. (12) leads to

$$I_+(z) = I_+(0)[1 + (z\gamma|A_0|^2)^2],$$
$$I_-(z) = I_+(0)(z\gamma|A_0|^2)^2. \tag{23}$$

Equations (23) become invalid when $I_\pm$ grows to be comparable to $|A_0|^2$.

In the normal-dispersion case, I_+ and I_- exhibit in-phase oscillations with the propagation distance, with the period $1/k(\omega')$, which is longer at the lower frequency. In the anomalous-dispersion case, $I_+(z) \sim I_-(z) \sim I_+(0)(1/4)(\gamma|A_0|^2)^2 \exp(2|k|z)/|k|^2$ at large distance with exponential growth caused by the gain of MI.

Figures 9 and 10 show the spectral evolution in the case of FWM induced by a probe of finite bandwidth for the cases of normal and anomalous dispersion, respectively, by assuming a Gaussian probe spectrum: $\Delta S(\omega, 0) \propto \exp\{-[(\omega - \omega')/\Delta\omega]^2\}$. With the above analysis for a narrow-bandwidth probe the qualitative behavior can be

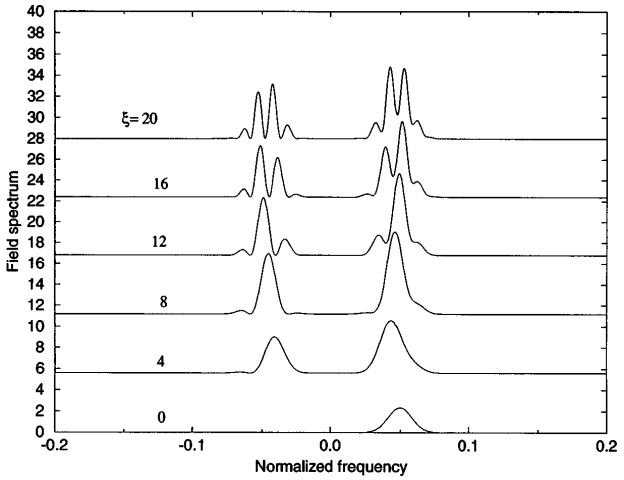

Fig. 9. Spectral evolution at different distances in the normal-dispersion region for an asymmetric input spectrum corresponding to FWM with a noisy probe. The noise spectrum is centered at 0.05 with a FWHM of 0.02; other parameters are identical to those of Fig. 1.

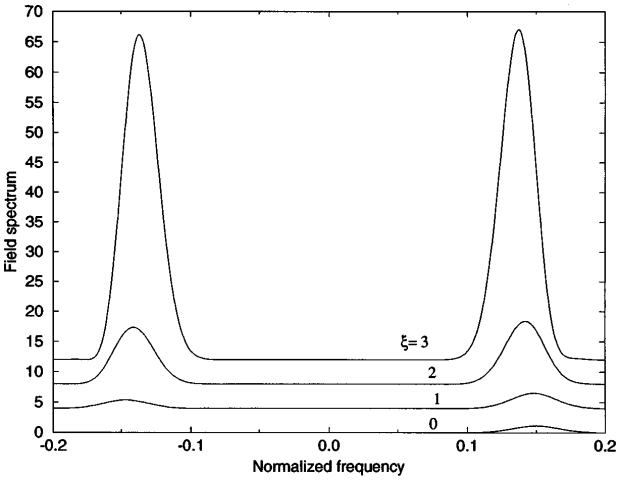

Fig. 10. Same as Fig. 9, except that the noise spectrum is centered at 0.15 with a FWHM of 0.04 and the GVD is anomalous.

understood easily because the spectrum can be linearly decomposed into the problem of many independent narrow-bandwidth probes. In the normal-dispersion region a spectral wing is generated at the symmetric position to the probe. The intensity oscillates with propagation distance initially. As each frequency component has a different oscillation period and a different initial intensity, the wings will be shifted and split to develop fringes. The average oscillation with distance will be saturated as more and more fringes appear because the fringes are all out of phase with one another. In fact, for large distance, the envelope of the two wings will settle down at the frequencies around $\pm\omega'$, with an average intensity of $\propto[1 + (\gamma|A_0|^2)^2/k^2(\omega)]\exp -[(\omega - \omega')/\Delta\omega]^2$ and $\propto[(\gamma|A_0|^2)^2/k^2(\omega)]\exp -[(\omega + \omega')/\Delta\omega]^2$, respectively. But it is the inverse width of the fringes under the envelope that gives the approximate correlation time. Thus the coherence times of the noisy signal and idler keep increasing with propagation. In the anomalous-dispersion case MI will produce symmetric wings at large distances. Because the gain peak is at $\pm(2\gamma|A_0|^2/\beta_2)^{1/2}$, the wings will be pulled toward this frequency position as they grow with distance.

Note that in both the normal- and the anomalous-dispersion cases the spectrum of the generated idler is not simply the mirror image of the input spectrum of the signal. This is due to the effect of GVD on the process of FWM. From a practical point of view this phenomenon implies that the midsystem spectral inversion by FWM in a dispersion-shifted fiber, a technique proposed recently for compensation of dispersion in fiber-optic communication systems,[15] can be affected by the residual dispersion in the dispersion-shifted fiber.

6. CONCLUSION

The pump effects on the propagation of a stochastic field in a nonlinear dispersive medium were studied both analytically and numerically. Simple expressions were obtained for the evolution of the power spectrum and the RIN as propagation distance changes. It was found that, in the case of anomalous GVD, MI plays a dominant role at large distances, as expected, where both the power spectrum and the RIN grow exponentially according to the MI gain to achieve symmetric patterns about the pump frequency. Even for normal GVD the FWM effects are not negligible. Each sideband generates the other sideband at the FWM frequency, thus establishing correlations between frequencies symmetrically located about the pump frequency. This causes oscillations in the power spectrum (and the quadratic growth near the pump frequency) and in the RIN with propagation distance. Because the oscillations are frequency dependent, fringe formations are found on the power spectrum and the RIN. The results were applied to the case of a symmetric input spectrum, which can correspond to laser intensity noise, and to the case of an asymmetric input spectrum, which can correspond to the FWM of a broadband probe in the presence of a cw pump.

ACKNOWLEDGMENTS

We thank a referee for bringing Refs. 12–14 to our attention. The research of G. P. Agrawal was supported by the U.S. Army Research Office under the University Research Initiative Program. That of C. J. McKinstrie and M. Yu was supported by the National Science Foundation under contract PHY-9057093, the U.S. Department of Energy (DOE) Office of Inertial Confinement Fusion under cooperative agreement DE-FC03-92SF19460, the University of Rochester, and the New York State Energy Research and Development Authority. The support of the DOE does not constitute an endorsement by the DOE of the views expressed in this paper.

REFERENCES

1. J. T. Manassah, Opt. Lett. **16,** 1638 (1991).
2. B. Gross and J. T. Manassah, Opt. Lett. **16,** 1835 (1991).
3. M. T. de Araujo, H. R. da Cruz, and A. S. Gouviea-Neto, J. Opt. Soc. Am. B **8,** 2094 (1991).
4. S. Ryu, Electron. Lett. **28,** 2212 (1992).
5. K. Kikuchi, IEEE Photon. Technol. Lett. **5,** 221 (1993).
6. J. N. Elgin, Opt. Lett. **18,** 10 (1992).
7. S. A. Akhmanov, V. A. Vysloukh, and A. S. Chirkin, *Optics of Femtosecond Laser Pulses* (American Institute of Physics, New York, 1992).
8. J. W. Goodman, *Statistical Optics* (Wiley, New York, 1985).
9. N. Wax, ed., *Noise and Stochastic Processes* (Dover, New York, 1954).
10. A. Hasegawa, *Optical Solitons in Fibers* (Springer-Verlag, Berlin, 1990).
11. G. P. Agrawal, *Nonlinear Fiber Optics*, 2nd ed. (Academic, Boston, Mass., 1989).
12. M. J. Potasek and B. Yurke, Phys. Rev. A **35,** 3974 (1987).
13. S. J. Carter, P. D. Drummond, M. D. Reid, and R. M. Shelby, Phys. Rev. Lett. **58,** 1841 (1987).
14. H. A. Haus and Y. Lai, J. Opt. Soc. Am. B **7,** 386 (1990).
15. A. H. Gnauck, R. M. Jopson, and R. M. Derosier, IEEE Photon. Technol. Lett. **5,** 104 (1993).
16. K. Kikuchi, IEEE Photon. Technol. Lett. **6,** 104 (1994).